a water molecule, a situation that should favour proton transfer from the W306 cation radical to the solvent. In contrast, W382 is buried in the hydrophobic interior of the protein. There is no potential proton acceptor within 5 Å of the ring nitrogen of W382, excluding the possibility of deprotonation of the cation radical. The indole ring of W359 is surrounded by both hydrophobic and polar amino acids. The ring nitrogen appears to be hydrogen bonded to a more buried water molecule that might assist deprotonation of the W359 cation radical; however, our experimental data with a time resolution of 10 ns, together with previous data on the W306F mutant[12], do not give any indication for a deprotonation of the W359 cation radical.

The different polarities of the tryptophan environments should be relevant for the energetics of the electron transfer, as the reduction potential of the $TrpH^{\bullet+}$/TrpH couple is higher in a hydrophobic protein environment than in water[14]. For this reason, there is likely to be some decrease of the free energy of the $TrpH^{\bullet+}$ states in the order W382, W359, W306, favouring radical localization on W306 already, before its deprotonation.

A reaction scheme quite different from Fig. 5 was proposed previously[9]. It assumed that a long-lived quartet state of $FADH^{\bullet}$ (formed by intersystem crossing from the initial excited doublet state) abstracts an electron from W306 in about 500 ns, and that the resulting cation radical $TrpH^{\bullet+}$ remains protonated. This mechanism is incompatible with our results which establish unambiguously that $TrpH^{\bullet+}$ is formed in less than 10 ns and deprotonates in about 300 ns. The origin of the disagreement is most probably that the previous scheme was based on studies[11,20,23] using 355-nm laser flashes or Xe flashes that could excite species other than $FADH^{\bullet}$ (for example, fully oxidized FAD; see ref. 24). Under our excitation conditions, $FADH^{\bullet}$ is the only species being excited.

In summary, we have reached a consistent mechanism for the radical transfer during photoactivation of photolyase in which sequential electron transfer among amino-acid residues generates transient cation radicals before charge neutralization by proton release to the solvent. Thus, we conclude that charge compensating simultaneous proton transfer is not a prerequisite for intraprotein radical transfer. A definitive answer to the question of whether long-range radical transfer in other enzymes proceeds through a similar mechanism may require time-resolved methods to selectively monitor electron transfer, H-atom transfer and protonation/deprotonation events.

Our results on the activation of DNA photolyase from *E. coli* may be relevant for the other photolyases (class I and class II)[10] and also for the cryptochrome blue-light receptors in plants and animals, which are flavoproteins similar in sequence to photolyases[25]. Indeed, inspecting the aligned amino-acid sequences[10] of known photolyases and cryptochromes, we noticed that the tryptophan residues W382, W359 and W306 are uniformly conserved. This observation suggests that the electron transfer chain described here is involved in the function of all photolyases, and of blue light receptors as well. □

Received 30 December 1999; accepted 10 January 2000.

1. Stubbe, J. & van der Donk, W. A. Protein radicals in enzyme catalysis. *Chem. Rev.* **98,** 705–762 (1998).
2. Uhlin, U. & Eklund, H. Structure of ribonucleotide reductase protein R1. *Nature* **370,** 533–539 (1994).
3. Sjöberg, B.-M. The ribonucleotide reductase jigsaw puzzle: a large piece falls into place. *Structure* **2,** 793–796 (1994).
4. Siegbahn, P. E. M., Blomberg, M. R. A. & Crabtree, R. H. Hydrogen transfer in the presence of amino acid radicals. *Theor. Chem. Acc.* **97,** 289–300 (1997).
5. Siegbahn, P. E. M., Eriksson, L., Himo, F. & Pavlov, M. Hydrogen atom transfer in ribonucleotide reductase (RNR). *J. Phys. Chem.* **102,** 10622–10629 (1998).
6. Cukier, R. I. & Nocera, D. G. Proton coupled electron transfer. *Annu. Rev. Phys. Chem.* **49,** 337–369 (1998).
7. Page, C. C., Moser, C. C., Chen, X. & Dutton, P. L. Natural engineering principles of electron tunnelling in biological oxidation-reduction. *Nature* **402,** 47–52 (1999).
8. Sancar, A. No "end of history" for photolyases. *Science* **272,** 48–49 (1996).
9. Kim, S. -T., Heelis, P. F. & Sancar, A. Role of tryptophans in substrate binding and catalysis by DNA photolyase. *Methods Enzymol.* **258,** 319–343 (1995).
10. Yasui, A. & Eker, A. P. M. in *DNA Damage and Repair, Vol. 2: DNA Repair in Higher Eukaryotes* (eds Nickoloff, J. A. & Hoekstra, M. F.) 9–32 (Humana, Totowa, 1998).
11. Heelis, P. F., Okamura, T. & Sancar, A. Excited-state properties of *Escherichia coli* DNA photolyase in the picosecond to millisecond time scale. *Biochemistry* **29,** 5694–5698 (1990).
12. Li, Y. F., Heelis, P. F. & Sancar, A. Active site of DNA photolyase: tryptophan-306 is the intrinsic hydrogen atom donor essential for flavin radical photoreduction and DNA repair *in vitro*. *Biochemistry* **30,** 6322–6329 (1991).
13. Eker, A. P. M., Yajima, H. & Yasui, A. DNA photolyase from the fungus *Neurospora crassa*. Purification, characterization and comparison with other photolyases. *Photochem. Photobiol.* **60,** 125–133 (1994).
14. Tommos, C., Skalicky, J. J., Pilloud, D. L., Wand, A. J. & Dutton, P. L. *De novo* proteins as models of radical enzymes. *Biochemistry* **38,** 9495–9507 (1999).
15. Solar, S., Getoff, G., Surdhar, P. S., Armstrong, D. A. & Singh, A. Oxidation of tryptophan and N-methylindole by $N_3^{\bullet}$, $Br_2^{\bullet-}$, and $(SCN)_2^{\bullet-}$ radicals in light- and heavy-water solutions: A pulse radiolysis study. *J. Phys. Chem.* **95,** 3636–3643 (1991).
16. Aubert, C., Mathis, P., Eker, A. P. M. & Brettel, K. Intraprotein electron transfer between tyrosine and tryptophan in DNA photolyase from *Anacystis nidulans*. *Proc. Natl Acad. Sci. USA* **96,** 5423–5427 (1999).
17. Aubert, C., Brettel, K., Mathis, P., Eker, A. P. M. & Boussac, A. EPR detection of the transient tyrosyl radical in DNA photolyase from *Anacystis nidulans*. *J. Am. Chem. Soc.* **121,** 8659–8660 (1999).
18. Cleland, W. W., O'Leary, M. H. & Northrop, D. B. *Isotope Effects on Enzyme-Catalyzed Reactions* (Univ. Park Press, Baltimore, London, Tokyo, 1977).
19. Eigen, M. Proton transfer, acid-base catalysis, and enzymatic hydrolysis Part I: elementary processes. *Angew. Chem. Internat. Edn.* **3,** 1–19 (1964).
20. Okamura, T., Sancar, A., Heelis, P. F., Hirata, Y. & Mataga, N. Doublet-quartet intersystem crossing of flavin radical in DNA photolyase. *J. Am. Chem. Soc.* **111,** 5967–5969 (1989).
21. Park, H. W., Kim, S. T., Sancar, A. & Deisenhofer, J. Crystal structure of DNA photolyase from *Escherichia coli*. *Science* **268,** 1866–1872 (1995).
22. Cheung, M. S., Daizadeh, I., Stuchebrukhov, A. A. & Heelis, P. F. Pathways of electron transfer in *Escherichia coli* DNA photolyase: Trp^{306} to FADH. *Biophys J.* **76,** 1241–1249 (1999).
23. Kim, S. T., Sancar, A., Essenmacher, C. & Babcock, G. T. Time-resolved EPR studies with DNA photolyase: excited-state $FADH^0$ abstracts an electron from Trp-306 to generate $FADH^-$, the catalytically active form of the cofactor. *Proc. Natl Acad. Sci. USA* **90,** 8023–8027 (1993).
24. Gindt, Y. M. *et al.* Origin of the transient electron paramagnetic resonance signals in DNA photolyase. *Biochemistry* **38,** 3857–3866 (1999).
25. Cashmore, A. R., Jarillo, J. A., Xu, Y. -J. & Liu, D. Cryptochromes: blue light receptors for plants and animals. *Science* **284,** 760–765 (1999).
26. Martin, J.-L. & Vos, M. H. Femtosecond measurements of geminate recombination in heme proteins. *Methods Enzymol* **232,** 416–430 (1994).
27. Heelis, P. F., Deeble, D. J., Kim, S. T. & Sancar, A. Splitting of cys-syn cyclobutane thymine–thymine dimers by radiolysis and its relevance to enzymatic photoreactivation. *Int. J. Radiat. Biol.* **62,** 137–143 (1992).
28. Guex, N. & Peitsch, M. N. SWISS-MODEL and the Swiss-PdbViewer: An environment for comparative protein modeling. *Electrophoresis* **18,** 2714–2723 (1997).

Acknowledgements

We thank A. Yasui for providing us with the *E. coli* photolyase expression construct; P. Barth and P. L. Dutton for helpful discussions; and T. A. Mattioli for critical reading of the manuscript. M.H.V. is supported by CNRS.

Correspondence and requests for materials should be addressed to K.B. (e-mail: brettel@dsvidf.cea.fr).

Engineering stability in gene networks by autoregulation

Attila Becskei & Luis Serrano

EMBL, Structures & Biocomputing, Meyerhofstrasse 1, Heidelberg D-69012, Germany

The genetic and biochemical networks which underlie such things as homeostasis in metabolism and the developmental programs of living cells, must withstand considerable variations and random perturbations of biochemical parameters[1–3]. These occur as transient changes in, for example, transcription, translation, and RNA and protein degradation. The intensity and duration of these perturbations differ between cells in a population[4]. The unique state of cells, and thus the diversity in a population, is owing to the different environmental stimuli the individual cells experience and the inherent stochastic nature of biochemical processes (for example, refs 5 and 6). It has been proposed, but not

demonstrated, that autoregulatory, negative feedback loops in gene circuits provide stability[7], thereby limiting the range over which the concentrations of network components fluctuate. Here we have designed and constructed simple gene circuits consisting of a regulator and transcriptional repressor modules in *Escherichia coli* and we show the gain of stability produced by negative feedback.

To test the role of negative feedback in the stability of gene networks, we first designed simple gene circuits based on simple control systems (Fig. 1c, d). To construct the autoregulatory system, the tetracycline repressor (TetR) of the transposon Tn10 was fused to the green fluorescent protein (EGFP) (TetR–EGFP) and placed downstream of the lambda promoter containing two tetracycline operators (Fig. 2a). As controls, the unregulated counterparts were obtained by slight modification of this system. In this way, differences among the systems could be neglected, while the feedback was eliminated (Fig. 2b, c).

To get a quantitative measure of the stability of our systems, a linear stability analysis was performed using differential equation models of gene circuits. The use of quantitative stability analysis allows modelling of biological processes in their natural context. When a particular process is selected for examination *in vivo*, its description is biased by the impact of the unique state of the cell, so it cannot be fully characterized as a separate entity isolated from the perturbations of the biochemical network of the cell. Actually, comparative stability analysis takes the cellular perturbations into account. The value of the stability (S) is obtained by the linearization of the equations around the steady state. The absolute values of stability of the unregulated (1) and autoregulatory (2) systems were compared as the ratio of the stability (3) of the two systems.

$$S_{\text{unreg}} = f'_{\text{unreg}}(R^*) = -k_{\text{deg}} \tag{1}$$

$$S_{\text{auto}} = f'_{\text{auto}}(R^*) = -\frac{nk_pPk_Iak_r}{(1+k_pP+k_rR^*)^2} - k_{\text{deg}} \tag{2}$$

$$S_r = \frac{S_{\text{auto}}}{S_{\text{unreg}}} \tag{3}$$

Where R is the concentration of the repressor (R^* at the steady state), P is the concentration of the RNA polymerase, k_p and k_r are the binding constants of the polymerase and the repressor, respectively, k_I is the promoter isomerization rate from closed to initiating complex, a is the proportionality constant between the mRNA and protein concentration, k_{deg} is the degradation rate of the repressor and n is the gene copy number.

It is apparent that for all positive values of parameters and steady state concentrations the stability is higher in the autoregulatory system. For the biochemical parameters of the systems constructed here, the autoregulatory system shows a twofold increase in stability over the unregulated one. Varying the parameters within a range of values with biological significance demonstrates that the stability gain by negative feedback is preserved. However, it decreases considerably when the binding constant for the repressor or the transcription rate is very low, especially when the repressor has a short half-life (Fig. 1a, b). Actually, low repression factor and low concentration of repressor affect the essential property of negative feedback. A detailed mathematical analysis shows that conditions can be found when the degree of stability of the two systems converges while the parameters are unchanged. However, the autoregulatory system is generally superior, and only equal to the unregulated system under certain conditions. To simulate the unique perturbation states of cells, random perturbations were applied to the steady state in a cell population, which resulted in a variation of the actual concentration of the transcription factor around the steady state in the population (Fig. 1). However, the distribution is narrower in the autoregulatory system owing to the higher stability.

In the second step, we analysed the degree of variability in the expression of the TetR–EGFP by fluorescence microscopy in the autoregulatory and three unregulated systems. Coefficient of variation (V_c) was used as a measure of variability. The expression of the TetR–EGFP in the autoregulatory loop is characterized by a low steady-state level and high degree of homogeneity (Fig. 2a), with a V_c of 6–9% (Fig 3a, column A). The narrow distribution is not specific to very low copy plasmids. Essentially the same V_c, values were observed in cell populations harbouring very low, middle and high copy number plasmids (data not shown).

The negative feedback is expected to be maintained if a low concentration of inducer is added to the medium. When anhydrotetracycline (atc) is added at very low concentration (1 ng ml^{-1}), V_c stays below 10%. However, a transition from the autoregulatory to the first unregulated system occurs at higher inducer concentrations owing to the reduction of feedback repression (Fig. 3b).

As predicted, decreasing the affinity of the repressor by a mutation[8] increases the variability in the second system (Fig. 2b) and the steady-state concentration of the fusion protein. The variability was comparable to that encountered in the autoregulatory system when high concentrations of inducer were added (~20%, Fig. 3a). The significant difference of the steady-state concentrations is because of the high binding affinity of the wild-type TetR, which is also involved in the stabilization of feedback.

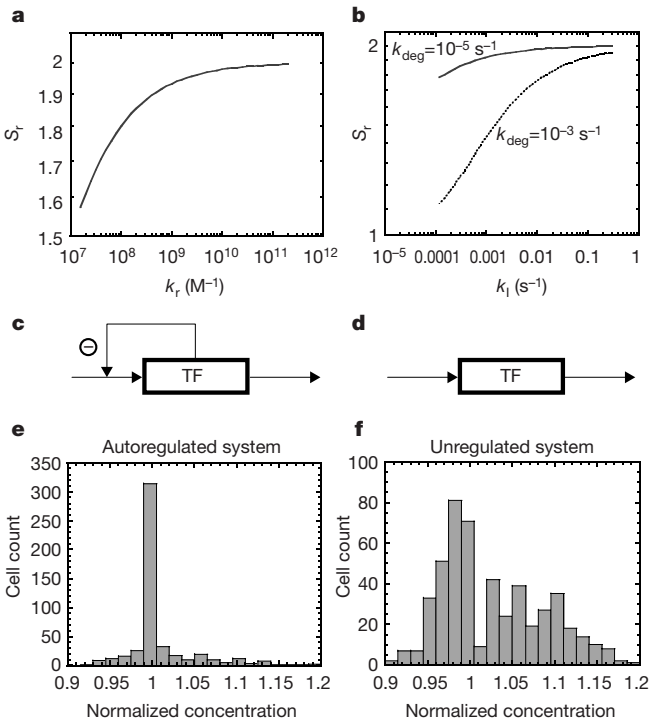

Figure 1 Stability properties of gene circuits. **a**,**b**, For calculating the value of relative stability (S_r, equation 3), the parameters of the system are: $P = 100$ nM, $k_p = 1.5 \times 10^{10}$ M^{-1}, $k_I = 0.3$ nM s^{-1}, $n = 3$, $a = 3.3$, $k_r = 2 \times 10^{11}$ M^{-1}, $k_{deg} = 10^{-5}$ s^{-1}, while one parameter is selected for independent variable: k_r (**a**) or k_I (**b**). In *E. Coli* k_I ranges from 10^{-4} to 1 synthesized RNAs[24]. **c–d**, Control theoretical diagrams for negative feedback (**c**) and unregulated (**d**) systems containing a transcription factor (TF). Inflow arrow stands for the rate of synthesis, the outflow arrow for the rate of degradation. **e–f**, Numerical simulation is given for both systems, where the actual concentration of each cell is normalized by the calculated steady-state value.

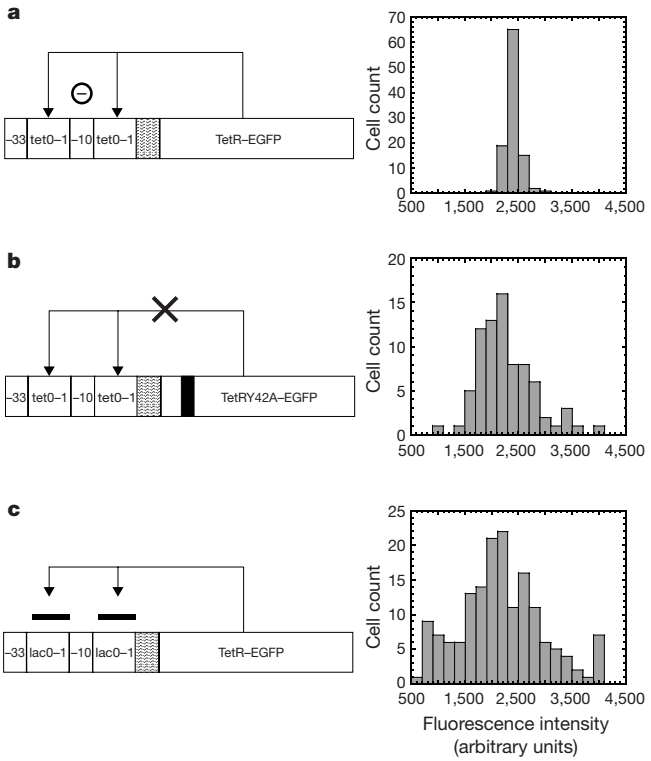

Figure 2 Gene circuits and corresponding typical distributions of fluorescence intensities. Each circuit consists of the following units: operator at position V, –33 hexamer, operator at position IV, –10 hexamer, untranslated region, fusion protein. GFP fluorescence intensity is denoted by arbitrary units in the histograms which corresponds to intensities of a 12-bit (4,096 grey level) image. The mean values of the three systems were normalized from different exposure times. Relative mean values (r.m.v.) are given for each distribution. **a**, Autoregulatory system in DH5α cells; r.m.v. = 1. **b**, The repressor was mutated (Y42A) in the DNA-binding domain to obtain the unregulated system in DH5α cells; r.m.v. = 38. **c**, Unregulated system obtained by operator replacement in DH5αZ1 cells. Sample is taken after induction by IPTG; r.m.v. = 14.

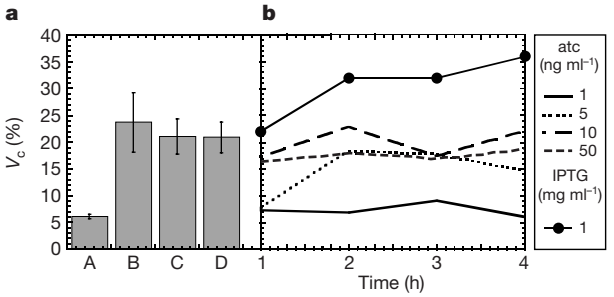

Figure 3 Variability in classical and autoregulatory systems. **a**, Mean coefficients of variation were calculated from three independent experiments using independent transformants, and were considered as simple statistical variables to calculate standard errors indicated on error bars. This characterizes the range of variability of independent experiments. Column A, the autoregulatory system; column B, an EGFP expression vector under the regulation of chromosomal TetR; column C, the operator-replaced unregulated system (Fig. 2c) after addition of 1 mM IPTG; column D, the mutant-repressor unregulated system (Fig. 2b). The same exposure times were applied to take the images for statistical analysis. **b**, Variability in the course of time after induction. The autoregulatory system is induced by different atc concentrations. The unregulated system (Fig. 2c) is induced by IPTG. The scale for V_c is the same in **a** and **b**.

In both systems, there is a residual binding of the repressor to the operator, as both the TetR–atc complex and the TetRY42A mutant have low binding affinities to the operator[8,9]. As a third model for an unregulated system, the tet operator was replaced by the lac operator (Fig. 2c), so only a negligible nonspecific protein–DNA interaction remains. The expression of TetR–EGFP was induced by saturating isopropyl-β-D-thiogalactopyranoside (IPTG) concentration (1 mM) to minimize stochastic induction phenomena observed at subsaturating concentrations of inducer[6,10]. The distribution of the fluorescence intensities was broader than in any other construct (Fig. 2c); two hours after induction V_c was above 30% (Fig. 3b). Furthermore, we were able to examine whether long-term expression affects the variability. High variability was observed in both the long-term expression of the TetRY42A–EGFP mutant, where the steady state is continuously maintained during bacterial growth, and in the short-term expression of TetR–EGFP, where expression is induced by release of Lac repressor from the operators (Fig. 3b).

Although V_c is appropriate to compare the variation of cell populations independent of the magnitude of their means, we checked that the homogeneity is not merely a consequence of the low steady-state level of TetR–EGFP in the autoregulatory system. This was done by two different experiments. First, samples were taken at different time intervals shortly after induction from the third unregulated system (Fig. 2c). Samples were selected that have similar mean fluorescence intensities to those in the autoregulatory system. There was a considerable difference in variability between the unregulated ($V_c \approx 20\%$) and the autoregulatory systems ($V_c \approx 6\%$) while their means were equal (Fig. 3a). Second, we measured EGFP expression under the control of chromosomal TetR. TetR controlled vector systems provide the most tightly regulated and evenly distributed expression presently available[11]. At low inducer concentrations (3–5 ng ml^{-1} atc), the mean EGFP fluorescence intensity of the cell population is roughly equal to that of the autoregulatory system. However, it shows about three-fold higher variability compared with the autoregulatory system (Fig. 3a).

Finally we investigated the possibility of dosage compensation by negative feedback loop. We monitored the mean expression level of luciferase produced by TetR–EGFP/luc bicistronic transcription unit when using low, medium and high copy plasmids (3–4, 20–30, 50–70 copies per cell, respectively). When the mean luminescence activity of the low copy system is normalized to one, the values for middle and high copy system are 2.6 ± 0.26 and 4.8 ± 0.69, respectively. These data could be explained by the analytical description of the steady state, which is a power function of the plasmid copy number. Thus, autoregulation might contribute to dosage compensation but additional mechanisms are necessary to keep the protein at a constant concentration, independent of gene copy number. Indeed, both negative feedback and postranscriptional regulation participate in the dosage compensation of histone genes in yeast[12,13].

Recent works of integrative theoretical–experimental approach have shed light on some of the basic principles of the functioning of gene networks[14,15]. Here we have focused on the stability by autoregulation proving its superiority to unregulated systems. In fact, roughly 40% of known transcription factors in *E. coli* negatively autoregulate themselves[16]. Reduced or increased amounts of the same transcriptional regulator can be the cause of severe developmental disorders[17]. Negative feedback provides a mechanism to ensure a homogeneous distribution of a transcriptional repressor within optimal concentration limits. Under certain conditions, however, the stability of the autoregulatory system could approach that of the classical system. Variability can be advantageous for adaptation[18], stability for homeostasis. □

Methods

Analysis of stability

Equations 4 and 5 are based on thermodynamic–kinetic principles[19] and the following data:

$$f_{\text{unreg}}(R) = \frac{dR}{dt} = n\frac{k_p P}{1 + k_p P}k_t a - k_{\text{deg}}R \quad (4)$$

$$f_{\text{auto}}(R) = \frac{dR}{dt} = n\frac{k_p P}{1 + k_p P + k_r R}k_t a - k_{\text{deg}}R \quad (5)$$

(1) The TetR exists only in the form of dimers in bacterial cells owing to the very high dimerization constant ($k_d = 4.8 \times 10^{13}$; ref. 20), so a linear correlation can be assumed between the concentration of TetR transcript and that of the dimer. Thus, the dimer concentration is half of that of the transcript. (2) Only the operator at position IV contributes significantly to repression. Its repression factor is around 100 times higher than that of the operator at position V (see legend of Fig. 2). The strength of the promoters containing the tetO-1 and lacO-1 operators are approximately the same[21]. (3) The RNA polymerase and the TetR bind mutually exclusively to the operator (V)[21]. The steady-state level of the repressor (R^* when $f(R) = 0$) is a linear function of gene copy number in unregulated systems, but a square-root function in autoregulatory systems. The stability value is obtained by the Taylor expansion of the $f(R^*+\eta)$ where η is the perturbation: $f(R^* + \eta) = f(R*) + \eta f'(R*) + O(\eta^2)$. $O(\eta^2)$ denotes quadratically small terms in η and can be neglected. The magnitude of $f'(R^*)$ determines the decay rate of the perturbation[22]. For numerical simulations, random values of same relative range were taken for η to perturb the steady state of the circuits at random time intervals, and the actual concentration of the transcription factor was taken from a population of 500 cells.

Strains, growth conditions and media

The *E.coli* DH5α and DH5αZ1 strains were used in all experiments. DH5αZ1 is derived from DH5α by chromosomal integration of transcriptional repressors LacI and TetR and also a spectinomycine resistance (Sp^r) marker[23]. DH5αZ1 produces ~3,000 molecules of LacI and ~7,000 molecules of TetR per cell[23]. Cells were grown in Luria broth with 30 μg ml^{-1} kanamycin and 50 μg ml^{-1} streptomycine. Cells from overnight cultures were diluted 1:100 and grown at 25 °C. Expression was induced at early log phase by addition of different atc (1–100 ng ml^{-1}) concentrations or IPTG at saturating concentration (1 mM) depending on the system. Samples for examination were taken from mid-log cultures.

Gene circuit construction

TetR, EGFP and firefly luciferase were amplified by polymerase chain reaction. The TetRY42A mutant was created by site-directed mutagenesis introducing a GCC triplet coding for alanine and verified by sequencing. The fusion protein is constructed from amino terminally positioned TetR or TetRY42A, a linker (with amino-acid sequence GENLYFQSGGA) and a carboxy terminally positioned EGFP. The tetO-1 and the lacO-1 regulatory units were cloned from pZE21MCS-1 and pZE22MCS-1. The regulatory and repressor modules were cloned into the very low copy plasmid pZS*21MCS-1 and in the case of the autoregulatory system the origin of replication was also changed to p15A and ColE1 to yield middle and high copy numbers per cell. To construct the bicistronic transcription unit the upstream TetREGFP module was ligated to luciferase separated by a ribosomal binding site and luciferase activity was measured as described[23].

Microscopy and statistical analysis

Bacteria were pelleted, washed and resuspended in PBS containing 50 μg ml^{-1} chloramphenicol to stop further protein synthesis. For microscopic examination, 10 μl of 1.5% agar was dropped on the microscope slide to form a thin layer. Immediately after drying, 1 μl of cell suspension was pipetted onto it and covered with a coverslip. Microscopy was carried out using a Leica DMIRB/E microscope equipped with a highly light-sensitive Hamamatsu C4742-95 digital CCD camera and an automatic light shutter. A Chroma GFP 513852 photocube transmitting a wavelength of 485–495 nm was used to stimulate GFP fluorescence. Fluorescent images of single fields of cells were obtained using a phase contrast ×63/1.32 oil-immersion lens with exposure times in a range between 10 and 4,000 ms. No detectable autofluorescence of control cells was observed in this range. Multiple exposures were taken of each field to assure that the fluorescence signal was within the range of the CCD camera. To compare variability of different systems having approximately the same mean fluorescence intensity, images were taken with the same exposure time on the same day. Relative mean values (r.m.v.) were calculated as the ratios of exposure times of two measurements. Transmission images were taken to identify all bacterial cells selected for fluorescence intensity measurement. For statistical analysis, mean GFP fluorescence intensities were measured using the Openlab 2.0.6 software. The mean fluorescence intensities of 75 to 150 individual cells from the central areas of single fields were quantified. To compare standard deviations in broad range of fluorescence intensities, we calculated coefficients of variation (V_c), which is not biased by the photobleaching of GFP. V_c is the simple ratio of standard deviation to mean at high sample numbers. Coefficients of variation of the same field were compared for different exposure times within the linear range. They are within the range of the standard error of V_c and are independent of exposure time and background fluorescence. The standard error of V_c is small for large samples.

Received 25 December 1999; accepted 13 April 2000.

1. Little, J. W., Shepley, D. P. & Wert, D. W. Robustness of a gene regulatory circuit. *EMBO J.* **18,** 4299–4307 (1999).
2. Barkai, N. & Leibler, S. Robustness in simple biochemical networks. *Nature* **387,** 913–917 (1997).
3. Alon, U., Surette, M. G., Barkai, N. & Leibler, S. Robustness in bacterial chemotaxis. *Nature* **397,** 168–171 (1999).
4. Ko, M. S., Nakauchi, H. & Takahashi, N. The dose dependence of glucocorticoid-inducible gene expression results from changes in the number of transcriptionally active templates. *EMBO J.* **9,** 2835–2842 (1990).
5. Nutt, S. L. *et al.* Independent regulation of the two Pax5 alleles during B-cell development. *Nat. Genet* **21,** 390–395 (1999).
6. Novick, A. & Weiner, M. Enzyme induction as an all-or-none phenomenon. *Proc. Natl Acad. Sci. USA* **43,** 553–566 (1957).
7. Savageau, M. A. Comparison of classical and autogenous systems of regulation in inducible operons. *Nature* **252,** 546–549 (1974).
8. Baumeister, R., Helbl, V. & Hillen, W. Contacts between Tet repressor and tet operator revealed by new recognition specificities of single amino acid replacement mutants. *J. Mol. Biol.* **226,** 1257–1270 (1992).
9. Lederer, T. *et al.* Tetracycline analogs affecting binding to Tn10-Encoded Tet repressor trigger the same mechanism of induction. *Biochemistry* **35,** 7439–7446 (1996).
10. Siegele, D. A. & Hu, J. C. Gene expression from plasmids containing the araBAD promoter at subsaturating inducer concentrations represents mixed populations. *Proc. Natl Acad. Sci. USA* **94,** 8168–8172 (1997).
11. Blau, H. M. & Rossi, F. M. Tet B or not tet B: advances in tetracycline-inducible gene expression. *Proc. Natl Acad. Sci. USA* **96,** 797–799 (1999).
12. Moran, L., Norris, D. & Osley, M. A. A yeast H2A-H2B promoter can be regulated by changes in histone gene copy number. *Genes Dev.* **4,** 752–763 (1990).
13. Osley, M. A. & Hereford, L. M. Yeast histone genes show dosage compensation. *Cell* **24,** 377–384 (1981).
14. Gardner, T. S., Cantor, C. R. & Collins, J. J. Construction of a genetic toggle switch in *Escherichia coli*. *Nature* **403,** 339–342 (2000).
15. Elowitz, M. B. & Leibler, S. A synthetic oscillatory network of transcriptional regulators. *Nature* **403,** 335–338 (2000).
16. Thieffry, D., Huerta, A. M., Perez-Rueda, E. & Collado-Vides, J. From specific gene regulation to genomic networks: a global analysis of transcriptional regulation in *Escherichia coli*. *Bioessays* **20,** 433–440 (1998).
17. Schedl, A. *et al.* Influence of PAX6 gene dosage on development: overexpression causes severe eye abnormalities. *Cell* **86,** 71–82 (1996).
18. Rutherford, S. L. & Lindquist, S. Hsp90 as a capacitor for morphological evolution. *Nature* **396,** 336–342 (1998).
19. Wolf, D. M. & Eeckman, F. H. On the relationship between genomic regulatory element organization and gene regulatory dynamics. *J. Theor. Biol.* **195,** 167–186 (1998).
20. Backes, H. *et al.* Combinations of the alpha-helix-turn-alpha-helix motif of TetR with respective residues from LacI or 434Cro: DNA recognition, inducer binding, and urea-dependent denaturation. *Biochemistry* **36,** 5311–5322 (1997).
21. Lanzer, M. & Bujard, H. Promoters largely determine the efficiency of repressor action. *Proc. Natl Acad. Sci. USA* **85,** 8973–8977 (1988).
22. Strogatz, S. H. *Nonlinear Dynamics and Chaos: With Applications in Physics, Biology, Chemistry, and Engineering* (Perseus, Boulder, CO, 1994).
23. Lutz, R. & Bujard, H. Independent and tight regulation of transcriptional units in *Escherichia coli* via the LacR/O, the TetR/O and AraC/I1–I2 regulatory elements. *Nucleic Acids Res.* **25,** 1203–1210 (1997).
24. Record JR., M. T., Reznikoff, W. S., Craig, M. L., McQuade, K. L. & Schlax, P. J. *E. coli and S. typhimurium: Cellular and Molecular Biology* (ed. Neidhardt, F. C.) 792–821 (American Society of Microbiology, Washington DC, 1996).

Acknowledgements

We thank H. Bujard for the plasmids; J. Rietdorf and R. Pepperkok for help with fluorescence microscopy; M. Diehl and D. Thieffry for discussions; and H. Domingues and R. Guerois for reading the manuscript. A.B. is supported by the Louis-Jeantet foundation.

Correspondence and requests for materials should be addressed to A.B. (e-mail: becskei@embl-heidelberg.de).